

An Analytical Solution for Slug-Tracer Tests in Fractured Reservoirs

Chao Shan and Karsten Pruess

Earth Sciences Division, Lawrence Berkeley National Laboratory

Berkeley, CA 94720, U.S.A.

Email: c_shan@lbl.gov

Abstract

The transport of chemicals or heat in fractured reservoirs is strongly affected by the fracture-matrix interfacial area. In a vapor-dominated geothermal reservoir, this area can be estimated by inert gas tracer tests, where gas diffusion between the fracture and matrix causes the tracer breakthrough curve (BTC) to have a long tail determined by the interfacial area. For water-saturated conditions, recent studies suggest that sorbing solute tracers can also generate strong tails in BTCs that may allow a determination of the fracture-matrix interfacial area. To theoretically explore such a useful phenomenon, this paper develops an analytical solution for BTCs in slug-tracer tests in a water-saturated fractured reservoir. The solution shows that increased sorption should have the same effect on BTCs as an increase of the diffusion coefficient. The solution is useful for understanding transport mechanisms, verifying numerical codes, and for identifying appropriate chemicals as tracers for the characterization of fractured reservoirs.

Key words: *analytical solution, long tail, breakthrough curve, fractured reservoir, and interfacial area.*

Introduction

Fluid flow and chemical transport in fractured porous media has been a research topic for decades. The topic is important because many geologic formations are fractured to some extent, and is also difficult because fracture networks can have quite diverse geometry (such as the direction, aperture, and density of fracture sets, and the number of fracture sets), with significant impact on flow and transport processes. Thus, it is crucial to obtain a clear geometric picture of a fractured reservoir for managing waste disposal, groundwater cleanup, or thermal-energy extraction. For example, in the design and operation of hot fractured rock (HFR) reservoirs, it is very important to estimate the heat transfer area between the fracture network and the matrix rock. An effective way to obtain this geometric information is to conduct an appropriate tracer test. Extensive studies on tracer transport in fractured porous media have been conducted in the context of nuclear and chemical waste disposal (e.g., Moreno, et al., 1996; Polak, et al., 2003). Based on these studies, mathematical models have been developed for analyzing tracer test data. Since naturally fractured reservoirs usually are very complex, an appropriate numerical code is usually needed.

However, numerical codes must be verified against analytical solutions before application to practical problems. Analytical solutions for contaminant transport in fractured porous media have been available since the early 1980s (Tang et al., 1981; Sudicky and Frind, 1982). The former paper is for a single fracture where the matrix is assumed to extend to infinity away from the fracture, while the latter is for the case of a set of parallel fractures with uniform fracture spacing and identical solute concentration at the entrance of the fractures. In both solutions the authors assumed a step change of

solute concentration at the fracture entrance. Such a boundary condition may be appropriate for analyzing contaminant migration away from waste disposal facilities. In a tracer test, however, this assumption is usually invalid; and instead we may assume a slug-like flux boundary condition at the fracture entrance. More recently, Moridis (2002) developed semianalytical solutions for radioactive or reactive solute transport in variably fractured layered media. His solutions are for more general cases and thus are relatively more complex. Here we use simplifying assumptions to develop a simple solution for a slug tracer test in a fractured rock under single-phase water flow conditions.

Theory

To simplify the problem, we assume that the system has a single set of identical plane, parallel fractures with a uniform fracture spacing, $2B$ [L], and a uniform fracture aperture, $2b$ [L]. We also assume that solute tracer is uniformly injected into the fractures at a constant pore velocity, v [L/T]. The tracer concentration applied at each fracture entrance is denoted by C_0 [M/L³]. Taking advantage of symmetry, we can restrict the solution to an elementary part of the system (one-half of a fracture and one-half of its adjacent matrix block) as shown in Figure 1. The z -axis is in the direction of the fracture, while the x -axis is perpendicular to the interface, pointing away from the fracture (Figure 1). The fracture is thus in the domain $-b \leq x \leq 0$ and $0 \leq z < \infty$; and the matrix is in the domain $0 \leq x \leq B$ and $0 \leq z < \infty$. The solid lines in Figure 1 represent zero-mass-flux boundaries. The aperture is assumed much smaller than the length of the fracture, and transport in the fracture is assumed one-dimensional along the fracture. The diffusive mass flux across the fracture-matrix interface is treated as a sink term in the

mass conservation equation for the fracture. We neglect any advective flow across the interface. By this assumption, there is no advection in the matrix; and mass transport in the matrix is only through diffusion perpendicular to the fracture-matrix interface. We ignore diffusion and adsorption inside the fracture, as well as any tracer decay. Reversible sorption in the matrix is accounted for by a retardation factor. Based on these assumptions, we use the following governing equations simplified from Sudicky and Frind (1982):

$$\frac{\partial C_R}{\partial t} + v \frac{\partial C_R}{\partial z} + \frac{q}{b\phi C_0} = 0 \quad (z \geq 0) \quad (1a)$$

$$\frac{\partial C_R'}{\partial t} - \frac{D'}{R'} \cdot \frac{\partial^2 C_R'}{\partial x^2} = 0 \quad (0 \leq x \leq B) \quad (1b)$$

where C_R and C_R' (both dimensionless) are the relative solute concentrations in the fracture and the matrix, respectively, which are defined by:

$$C_R = C / C_0; \quad C_R' = C' / C_0 \quad (1c)$$

Here C [M/L³] and C' [M/L³] represent the chemical concentrations in the fracture and matrix, respectively.

In (1a) and (1b), t [T] is time, q [M/L²/T] the diffusive mass flux across the fracture-matrix interface, ϕ the intrinsic porosity of the fracture, D' [L²/T] and R' the diffusion coefficient and retardation factor of the matrix, respectively. Both C_R and q are functions of z and t , i.e. $C_R(z, t)$ and $q(z, t)$. The relative concentration in the matrix, C_R' , depends on the migration distance in the fracture, z , as a parameter through the interface boundary conditions; in (1b) it is an explicit function of x and t only.

The following formulae are provided for estimating some parameters:

$$D' = \tau D^* \quad (2a)$$

$$R' = 1 + K_m \rho_b / \phi' \quad (2b)$$

where τ is the tortuosity of the matrix; D^* [L^2/T] is the chemical molecular diffusion coefficient in water, typically of order 10^{-9} m^2/s ; and K_m [L^3/M] is the matrix distribution coefficient (Freeze and Cherry, 1979). In (2b) ρ_b [M/L^3] and ϕ' are the bulk mass density and the porosity of the matrix, respectively.

We assume an initially solute-free condition, i.e., the chemical concentrations in the fracture and matrix are both zero at the beginning:

$$C_R(z, 0) = C_R'(x, 0) = 0 \quad (3)$$

Setting $t = 0$ at the start time of tracer injection, and assuming an injection period t_i [T], the boundary conditions for the fracture are:

$$C_R(0, t) = 1 \quad (0 < t < t_i); \quad C_R(0, t) = 0 \quad (t > t_i) \quad (4a)$$

$$C_R(\infty, t) = 0 \quad (4b)$$

One boundary condition for the matrix is:

$$\left(\frac{\partial C_R'}{\partial x} \right)_{x=B} = 0 \quad (5)$$

At the fracture-matrix interface, we must have:

$$C_R(z, t) = C_R'(0, t) \quad (6a)$$

$$q = -\phi' D' C_0 \left(\frac{\partial C_R'}{\partial x} \right)_{x=0} \quad (6b)$$

Sudicky and Frind (1982) gave a general solution for the above problem under a constant boundary concentration that is different from (4a). Although the superposition principle does not make much physical sense for a concentration boundary condition, the principle is mathematically valid for this case. Here we present an independent

derivation process in the Appendix for obtaining more confidence. The analytical solution for this problem is:

$$C_R = \begin{cases} 0 & (t \leq t_T) \\ \frac{2}{\pi} \int_0^\infty \frac{e^{\varepsilon_R} \varepsilon_A}{\varepsilon} d\varepsilon & (t > t_T) \end{cases} \quad (7a)$$

$$C_R' = \frac{1}{2\sqrt{\pi}} \sum_{n=1}^{\infty} (-1)^{n-1} \int_0^t \frac{1}{(t-\tau)^{3/2}} \left(x_{n1} e^{-x_{n1}^2/(4t-4\tau)} + x_{n2} e^{-x_{n2}^2/(4t-4\tau)} \right) C_R(\tau) d\tau \quad (7b)$$

where $\varepsilon [T^{-1/2}]$ is the integration variable, ε_R is given by (A19a) that can be simply written as:

$$\varepsilon_R = -\frac{t_T \varepsilon}{2\sqrt{t_F}} g_2(\sqrt{t_M} \varepsilon) \quad (8a)$$

and ε_A is given by

$$\varepsilon_A = \sin \left[\frac{\varepsilon^2}{2} (t_s - t + t_T) + \frac{t_T \varepsilon}{2\sqrt{t_F}} \cdot g_1(\sqrt{t_M} \varepsilon) \right] + \sin \left[\frac{\varepsilon^2}{2} (t - t_T) - \frac{t_T \varepsilon}{2\sqrt{t_F}} \cdot g_1(\sqrt{t_M} \varepsilon) \right] \quad (8b)$$

The three parameters, t_T , t_F , and t_M are defined by (A17a) through (A17c), respectively; x_{n1} , and x_{n2} in (7b) are defined by (A23). The two functions, g_1 and g_2 , and a special time, t_s , are defined as follows:

$$g_1(u) = \frac{\sinh(u) + \sin(u)}{\cosh(u) + \cos(u)} \quad (9a)$$

$$g_2(u) = \frac{\sinh(u) - \sin(u)}{\cosh(u) + \cos(u)} \quad (9b)$$

$$t_s = \begin{cases} t - t_T & (t < t_i + t_T) \\ t_i & (t \geq t_i + t_T) \end{cases} \quad (9c)$$

Since our practical interest is the variation of tracer concentrations in the fracture, we will only evaluate solution (7a) in the following.

The integrand in (7a) is oscillatory, and care is needed to obtain accurate results. We use the method of Gaussian quadrature, and integrate (7a) by parts in the following steps. Step 1, perform a substitution of variable using $u = \sqrt{t_M} \varepsilon$ (note that u is dimensionless); step 2, refine the integration of (7a) in the interval $0 \leq u \leq 6$ using a uniform step of 0.1; step 3, for $u > 6$, separately calculate the u coordinates corresponding to the zeros of the two sine functions in (8b), assuming $g_1(u) = 1$; step 4, split the integrand into two parts, each part containing a factor of a sine function in (8b); step 5, for $u \geq 6$, integrate each part interval by interval using the calculated u -coordinate corresponding to zeros of the sine function; and step 6, add all results of integration.

Since the integrand decrease exponentially for large u , we only calculated the integrals of 19 additional intervals for $u \geq 6$. We found that the result is sufficiently accurate for most times except when C_R becomes very small (e.g. less than 10^{-6}) at the BTC tail.

Results

There are four characteristic times that determine the relative concentration, C_R . Among them, the injection period, t_i is a known parameter; t_T , t_F , and t_M are three parameters representing the properties of the fractured formation. According to (A17a), t_T is the tracer transit (or travel) time to the observation point. Therefore, (7a) indicates that the tracer concentration at a specified calculation point will remain at its initial value (zero) before the transit time has elapsed. This is because, by assumption, tracer transport in the fracture is through advection only. At a given point, the shape of the BTC is thus affected by two other characteristic times, t_F and t_M . According to (A17b)

and (A17c), t_F and t_M can be thought of as two characteristic times for crossing the interface and the matrix block, respectively.

The Role of t_M

By definition (A17c), t_M is the product of B squared and the ratio R'/D' , both factors originating from (1b), the governing equation for the matrix. Thus t_M affects the tracer concentration distribution in the matrix, but does not affect the tracer concentrations in the fracture in most practical applications. Physically, t_M represents a time to reach the interior no-flow boundary of the matrix through diffusion; the longer the time, the later the boundary effect will come into play. Mathematically, t_M affects the concentration in fracture only through the two functions, $g_1(u)$ and $g_2(u)$ that are essentially a constant of unity for $u > 6$ (see Figure 2). In other words, t_M affects the solution only in the interval $0 < \varepsilon < \varepsilon_0$ where

$$\varepsilon_0 = 6 / \sqrt{t_M} = \frac{6}{B} \sqrt{\frac{D'}{R'}} \quad (10)$$

For a matrix block size of meters or larger, since $R' \geq 1$ and D' is usually less than 10^{-9} m²/s, the resulting value of ε_0 is on the order of or less than 10^{-4} s^{-1/2}. The integral in (7a) usually has negligible contribution in the interval 0 to 10^{-4} . We used the input parameters in Table 1 to calculate the BTCs at two different locations (two different values of t_T). At each location, we calculate the BTCs for three different values of fracture spacing ($2B$), keeping all other parameters fixed. Figures 3a and 3b show the comparisons of the calculated BTCs at a near location ($t_T = 0.5 t_i$) and a far location ($t_T = 10 t_i$), respectively. Both figures indicate that the effect of B (or t_M) is insignificant. At the near location ($t_T = 0.5 t_i$, figure 3a), a smaller B does cause a slight increase in concentration due to the

boundary effect. However, the transit time for a practical observation point is usually much larger than the injection period, t_i , which will not show such a difference. In figures 3a and 3b, the smallest B value is 5 cm. Although further decrease of B can cause larger differences in the BTC, very small B values are not of interest in practical applications. We should also remember the assumption of $B \gg b$ in deriving the solution.

The Role of t_F

In practice, the only parameter, apart from the tracer transit time t_T , which affects a fracture BTC is t_F . According to (A17b), t_F depends on the matrix diffusion coefficient (D') and the retardation factor (R') only through the product $D'R'$. This is a remarkable result in view of the fact that in the governing equation (1b) D' and R' appear only as the ratio D'/R' . The implication is that the impact of the matrix retardation factor on tracer concentrations in the fracture is the same as that of matrix diffusion coefficient. As far as solute concentrations in the fracture are concerned, reversible sorption in the matrix acts to effectively enhance matrix diffusion. This equivalence of matrix retardation factor to diffusion coefficient is demonstrated in Figure 4, where the BTCs at $t_T = 50 t_i$ are calculated using three different pairs of D' and R' with a constant product ($10^{-10} \text{ m}^2/\text{s}$). In Figure 4, the three calculated BTCs are identical because we maintained t_F a constant (10^8 s). Any reduction of t_F value implies a faster passage for tracer to enter the matrix, and thus causes a decrease of tracer concentration in the fracture during tracer injection but an increase of tracer concentration in the fracture after tracer injection.

In figure 5, we used constant values for t_i (10^4 s), t_T (10^6 s), and t_M (10^9 s) but varied t_F (10^9 s, 10^8 s, and 10^7 s). The decrease of the BTC peak and the increase of the BTC tail for decreasing t_F are both significant. For relatively large t_F (e.g., 10^9 s, or even 10^8 s), the BTC peak appears approximately at the time $t = t_T + t_i$. However, as t_F is decreased to 10^7 s, the BTC peak appears at a time that is significantly larger than $t_T + t_i$ (Figure 5).

Verification

TOUGH2 (Pruess, et al., 1999) is a numerical code for multiphase, multi-component flow, transport, and heat transfer problems. This code has been verified against many analytical solutions. Here we demonstrate the verification of TOUGH2 against the analytical solution (7a), using the problem parameters given in Table 2. A comparison with the analytical solution is given in Figure 6, showing excellent agreement for three different retardation factors. Note that TOUGH2 uses “mass fraction” instead of relative concentration. The results of the analytical solution were converted to mass fraction for the comparison.

Application

Although analytical solutions are usually too idealized for direct applications to field cases, here we offer some guidelines for the potential application to a simplified field condition. The main purpose of application is to inversely estimate the average fracture spacing, $2B$, and from that the fracture-matrix interfacial (heat or chemical transfer) area per unit volume.

The injection period, t_i , is known; and the breakthrough time (the tracer transit time), t_T , is observed in the tracer test. A BTC can be calculated by applying the known t_i and t_T , and an assumed t_F and t_M (e.g., 10^9 s) to (7a). Varying t_F , we obtain a set of BTCs. We then estimate t_F by fitting the observation data to the calculated BTCs. After t_F is estimated, we can calculate B by rewriting the definition formula, (A17b) into:

$$t_F = \frac{\phi_f^2 B^2}{\phi'^2 D' R'} \quad (11)$$

where ϕ_f is the fracture continuum (average) porosity defined by:

$$\phi_f = \frac{\phi b}{B + b} \approx \frac{\phi b}{B} \quad (12)$$

For a given fracture porosity, variation of fracture spacing results in different BTC tails. Figure 7 shows the effect of fracture spacing by using $\phi'/\phi_f = 10$, $D'R' = 10^{-9}$ m²/s, and fixed values for t_i , t_T , and t_M . We see that smaller fracture spacing causes larger fracture concentration in the BTC tail.

The fracture porosity ϕ_f can be estimated by means of the injection flux rate (q_i) and the pore velocity (v) by:

$$\phi_f = q_i / v = q_i \cdot t_T / z \quad (13)$$

The matrix porosity ϕ' can be estimated by laboratory tests on rock samples. The matrix tortuosity τ can be determined by laboratory tests or estimated using the Millington (1959) model:

$$\tau = (\phi')^{1/3} \quad (14)$$

Substituting this tortuosity and the known tracer molecular diffusion coefficient D^* into (2a) we obtain D' , the diffusion coefficient in the matrix. The bulk mass density, ρ_b , can be estimated by:

$$\rho_b = \rho_s(1 - \phi') \quad (15)$$

where ρ_s is the rock grain density (approximately 2650 kg/m³). The distribution coefficient of tracer in the matrix (K_m) can be determined by laboratory tests. Therefore, we can calculate the retardation factor, R' , using (2b). Finally we use (11) and obtain:

$$B = \frac{\phi'}{\phi_f} \sqrt{t_F D' R'} \quad (16)$$

The fracture-matrix interfacial area available for chemical or heat transfer per unit volume of the system is then $A/V = 1/(B + b) \cong 1/B$.

Conclusion

A simplified analytical solution for solute tracer migration in fractured reservoirs reveals some important facts. In most practical cases, the tracer concentration in the fracture is dependent on three characteristic times: the injection period t_i , the tracer transit time t_T , and the crossing-interface time t_F . The independence of the solution on another characteristic time t_M and the definition of t_F theoretically validate a new finding, namely, the retardation factor arising from reversible matrix sorption and the diffusion coefficient of the matrix have the same effect on tracer concentrations in the fracture. Although the diffusion coefficient is practically restricted, a wide range of retardation factors is practically available by using different chemical species as solute tracers. This equivalent effect thus provides the basis for using reversibly sorbing chemicals as tracers to test a fractured reservoir. The verification of a numerical code, TOUGH2, against the

analytical solution demonstrates excellent agreement. The analytical solution can also be useful as a screening tool for selecting solutes with appropriate sorption properties, and analyzing field data under simplified conditions. Such analysis can inversely estimate the two important parameters: the average fracture porosity and fracture spacing, from which the all-important fracture-matrix interfacial area per unit reservoir volume may be obtained.

Acknowledgment

This work was supported by the Assistant Secretary for Energy Efficiency and Renewable Energy, Office of Geothermal Technologies, of the U.S. Department of Energy under Contract No. DE-AC03-76SF00098. The authors would like to thank Dr. G. Moridis for reviewing the manuscript.

References

- Erdelyi, A. (1954), *Tables of Integral Transforms*, vol. I, 301 pp., McGraw-Hill, New York.
- Freeze, R. A., and J. A. Cherry (1979), *Groundwater*, 604 pp., Prentice-Hall, Englewood Cliffs, New Jersey.
- Moridis, G. J. (2002), Semianalytical solutions of radioactive or radioactive solute transport in variably fractured layered media, *Water Resour. Res.*, 38(12), 1310, doi: 10.1029/2001WR001028.
- Millington, R. J. (1959), Gas diffusion in porous media, *Science*, 130: 100-102.

- Moreno, L., B. Gylling, and I. Neretnieks (1997), Solute transport in fractured media – the important mechanisms for performance assessment, *J Contam. Hydrol.*, 25: 283-298.
- Polak, A., A. S. Grader, R. Wallach, and R. Nativ (2003), Tracer diffusion from a horizontal fracture into the surrounding matrix: measurement by computed tomography, *J Contam. Hydrol.*, 67: 95-112.
- Pruess, K., C. Oldenburg, and G. Moridis (1999), TOUGH2 User's Guide, Version 2.0, *Lawrence Berkeley National Laboratory Report*, LBNL-43134, Berkeley, CA.
- Skopp, J., and A. W. Warrick (1974), A two-phase model for the miscible displacement of reactive solutes in soils, *Soil Sci. Soc., Am. Proc.*, 38(4): 545-550.
- Sudicky, E. A., and E. O. Find (1982), Contaminant transport in fractured porous media: Analytical solutions for a system of parallel fractures, *Water Resour. Res.*, 18(6): 1634-1642.
- Tang, D. H., E. O. Find, and E. A. Sudicky (1981), Contaminant transport in fractured porous media: Analytical solution for a single fracture, *Water Resour. Res.*, 17(3): 555-564.
- Wylie, C. R., and L. C. Barrett (1982), *Advanced Engineering Mathematics*, 5th ed., 1103 pp., McGraw-Hill, New York.

Appendix A

To solve (1a) and (1b) against the initial and boundary conditions, we use the following definitions of the Laplace transforms:

$$w(z, s) = L\{C_R(z, t)\} = \int_0^{\infty} C_R e^{-st} dt \quad (\text{A1a})$$

$$w'(x, s) = L\{C_R'(x, t)\} = \int_0^{\infty} C_R' e^{-st} dt \quad (\text{A1b})$$

$$f(z, s) = L\{q(z, t)\} = \int_0^{\infty} q e^{-st} dt \quad (\text{A1c})$$

where s is the variable of the Laplace transform. Applying the Laplace transforms to the governing equations and boundary conditions, and using the initial condition, we obtain:

$$v \frac{dw}{dz} + sw = -\frac{f}{b\phi C_0} \quad (z \geq 0) \quad (\text{A2a})$$

$$D' \frac{d^2 w'}{dx^2} - R' s w' = 0 \quad (0 \leq x \leq B) \quad (\text{A2b})$$

$$w(0, s) = \frac{1}{s} (1 - e^{-t's}) \quad (\text{A3a})$$

$$w(\infty, s) = 0 \quad (\text{A3b})$$

$$\left(\frac{dw'}{dx} \right)_{x=B} = 0 \quad (\text{A4})$$

$$w(z, s) = w'(0, s) \quad (\text{A5a})$$

$$f = -\phi' D' C_0 \left(\frac{dw'}{dx} \right)_{x=0} \quad (\text{A5b})$$

Equation (A3a) is the Laplace transform (Erdelyi, 1954) of the boundary condition described by (4a). The general solution for (A2b) is:

$$w' = c_1 e^{a_1 x} + c_2 e^{-a_1 x} \quad (0 \leq x \leq B) \quad (\text{A6})$$

where c_1 and c_2 are two integral constants that are independent of x , and a_1 is defined by:

$$a_1 = \sqrt{\frac{R's}{D'}} \quad (\text{A7})$$

To satisfy (A4) we must have:

$$c_2 = c_1 e^{2a_1 B} \quad (\text{A8})$$

which simplifies (A6) into

$$w' = c_1 \left(e^{a_1 x} + e^{a_1(2B-x)} \right) \quad (0 \leq x \leq B) \quad (\text{A9})$$

Using (A9) in (A5b), we obtain:

$$c_1 = -\frac{f}{\phi' D' C_0 a_1 (1 - e^{2Ba_1})} \quad (\text{A10})$$

Substituting (A10) into (A9) and then using (A5a), we obtain:

$$f = a_2 w \quad (\text{A11a})$$

$$a_2 = \frac{\phi' D' C_0 a_1 (e^{2Ba_1} - 1)}{e^{2Ba_1} + 1} = \phi' D' C_0 a_1 \tanh(Ba_1) \quad (\text{A11b})$$

The result in (A11a) reduces (A2a) into:

$$v \frac{dw}{dz} + \left(s + \frac{a_2}{b\phi C_0} \right) w = 0 \quad (z \geq 0) \quad (\text{A12})$$

The general solution for (A12) is:

$$w = c_3 \exp\left(-\frac{s + a_2/(b\phi C_0)}{v} z\right) \quad (z \geq 0) \quad (\text{A13})$$

Apparently, (A13) satisfies the boundary condition, (A3b). Applying (A3a) to (A13) we obtain:

$$c_3 = \frac{1}{s} (1 - e^{-t's}) \quad (\text{A14})$$

The solutions for concentrations in the fracture and matrix in the Laplace domain are thus:

$$w = \frac{1}{s} (1 - e^{-t_i s}) \exp\left(-\frac{s + a_2 / (b\phi C_0)}{v} z\right) \quad (\text{A15a})$$

$$w' = \frac{e^{-(2B-x)a_1} + e^{-xa_1}}{1 + e^{-2Ba_1}} w \quad (\text{A15b})$$

To invert (A15a) we first rewrite it into:

$$w = \frac{1 - e^{-t_i s}}{s} \cdot \exp\left[-t_T s - t_T \sqrt{s/t_F} \tanh(\sqrt{t_M s})\right] \quad (\text{A16})$$

where

$$t_T = z/v \quad (\text{A17a})$$

$$t_F = \frac{\phi^2 b^2}{\phi'^2 D' R'} \quad (\text{A17b})$$

$$t_M = B^2 R' / D' \quad (\text{A17c})$$

In fact, t_T is the tracer transit (or travel) time from the fracture entrance to the point of calculation. Using the inversion evaluated by Skopp and Warrick (1974) we have (Sudicky and Frind, 1982):

$$L^{-1}\{\exp[-t_T s - t_T \sqrt{s/t_F} \cdot \tanh(\sqrt{t_M s})]\} = g(t) = \begin{cases} 0 & (t < t_T) \\ \frac{1}{\pi} \int_0^\infty \varepsilon \exp(\varepsilon_R) \cos(\varepsilon_I) d\varepsilon & (t > t_T) \end{cases} \quad (\text{A18})$$

where

$$\varepsilon_R = -\frac{t_T \varepsilon}{2\sqrt{t_F}} \left[\frac{\sinh(t_M \varepsilon) - \sin(t_M \varepsilon)}{\cosh(t_M \varepsilon) + \cos(t_M \varepsilon)} \right] \quad (\text{A19a})$$

$$\varepsilon_I = \frac{\varepsilon^2 (t - t_T)}{2} - \frac{t_T \varepsilon}{2\sqrt{t_F}} \left[\frac{\sinh(t_M \varepsilon) + \sin(t_M \varepsilon)}{\cosh(t_M \varepsilon) + \cos(t_M \varepsilon)} \right] \quad (\text{A19b})$$

In deriving (A18) we also used the following theorem (Wylie and Barrett, 1982, p. 428):

$$\text{If } L^{-1}\{\phi(s)\} = f(t), \text{ then } L^{-1}\{e^{-as} \phi(s)\} = f(t - a) \cdot u(t - a) \quad (\text{A20})$$

where $u(t - a)$ is the unit step function. Erdelyi (1954) gave the inversion for the other factor in (A16) as:

$$L^{-1}\left\{\frac{1 - e^{-t_i s}}{s}\right\} = \begin{cases} 1 & (0 < t < t_i) \\ 0 & (t > t_i) \end{cases} \quad (\text{A21})$$

Finally, applying the convolution theorem we obtain the solution for the concentration in the fracture as indicated in (7a). The solution for the matrix is slightly more complex. For the sake of completeness, we invert (15b) using the inversion for (15a) and the convolution theorem. To do this, we first rewrite the factor in (15b) by substituting in (A7) and conducting a series expansion:

$$\frac{e^{-(2B-x)a_1} + e^{-xa_1}}{1 + e^{-2Ba_1}} = \sum_{n=1}^{\infty} (-1)^{n-1} [e^{-x_{n1}\sqrt{s}} + e^{-x_{n2}\sqrt{s}}] \quad (\text{A22})$$

where

$$x_{n1} = (2Bn - x)\sqrt{R'/D'}; \quad x_{n2} = (2Bn - 2B + x)\sqrt{R'/D'} \quad (\text{A23})$$

We used the following formula in deriving (A23):

$$(1 + x)^{-1} = \sum_{n=1}^{\infty} (-1)^{n-1} x^{n-1} \quad (\text{A24})$$

Using the inversion formula (Erdelyi 1954):

$$L^{-1}\left\{e^{-a\sqrt{s}}\right\} = \frac{a}{2\sqrt{\pi}} \cdot \frac{e^{-a^2/(4t)}}{t\sqrt{t}} \quad (\text{A25})$$

we obtain:

$$L^{-1}\left\{\frac{e^{-(2B-x)a_1} + e^{-xa_1}}{1 + e^{-2Ba_1}}\right\} = \frac{1}{2t\sqrt{\pi t}} \sum_{n=1}^{\infty} (-1)^{n-1} (x_{n1} e^{-x_{n1}^2/(4t)} + x_{n2} e^{-x_{n2}^2/(4t)}) \quad (\text{A26})$$

Applying the convolution theorem we obtain the solution for the concentration in the matrix as indicated in (7b).

Table1. Base parameters used in Figures 3a, 3b and 4.

b (m)	t_i (s)	v (m/s)	D' (m ² /s)	ϕ	ϕ'	R'
0.005	28800	0.001	10^{-10}	1.0	0.05	1.0

Table 2. Specifications of TOUGH2 fracture-matrix problem.

Reservoir properties		
	Average (continuum) fracture permeability	$43.2 \times 10^{-15} \text{ m}^2$
	Matrix permeability	$1.9 \times 10^{-18} \text{ m}^2$
	Fracture porosity	1 %
	Matrix porosity	3 %
	Fracture spacing	1 m
	Solute diffusivity	$10^{-9} \text{ m}^2/\text{s}$
	Matrix tortuosity	0.1
Injection	Pore velocity	1 m/hr
	Tracer concentration	87.9 ppm
	Tracer injection period	8 hr
	Matrix retardation factor	1, 10, 100
Initial conditions		
	Pressure	60.0 bar
	Temperature	240 °C

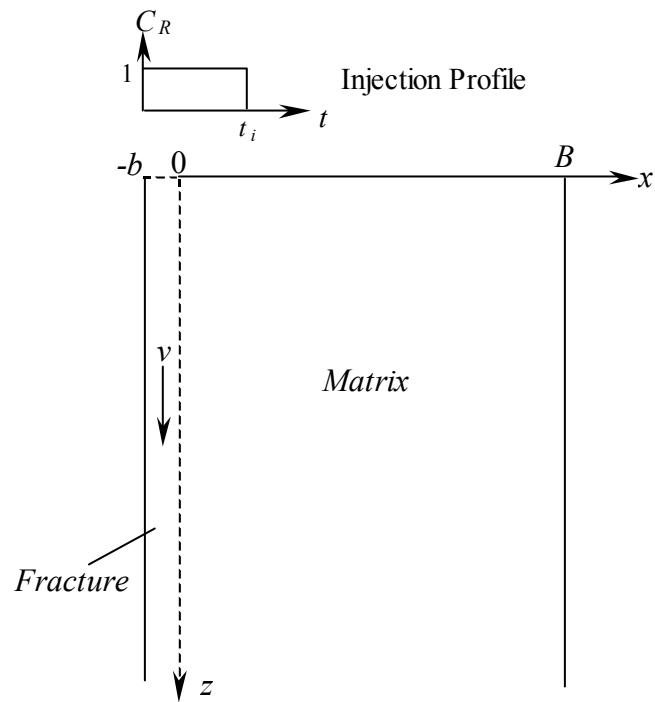


Figure 1. Schematic section of an elementary part of the parallel-fracture matrix system.

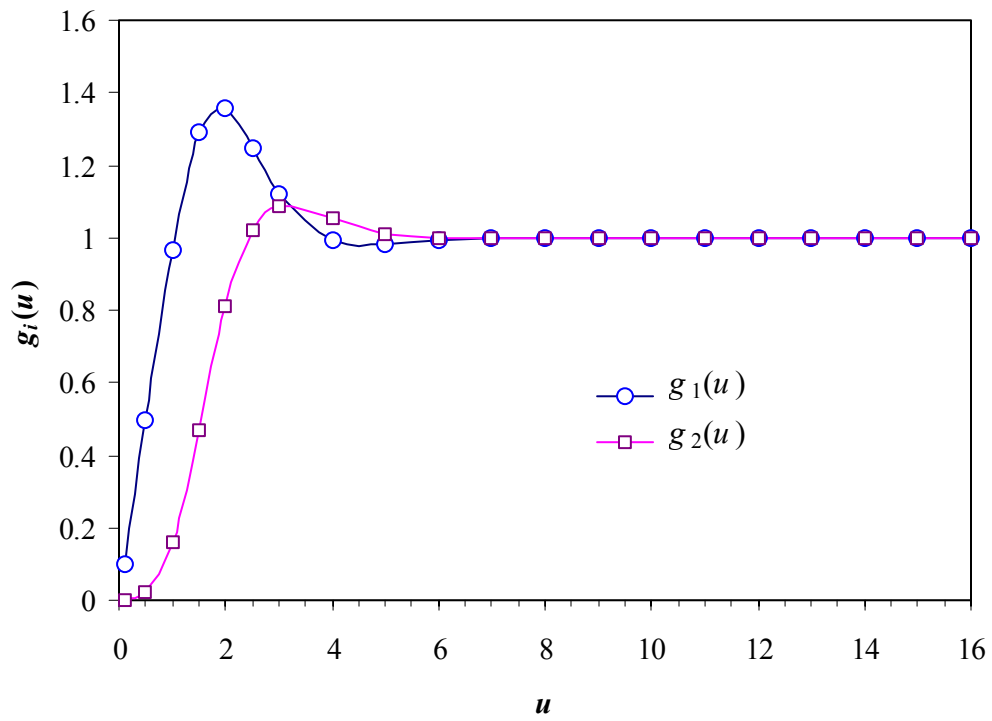


Figure 2. The functions, $g_1(u)$ and $g_2(u)$.

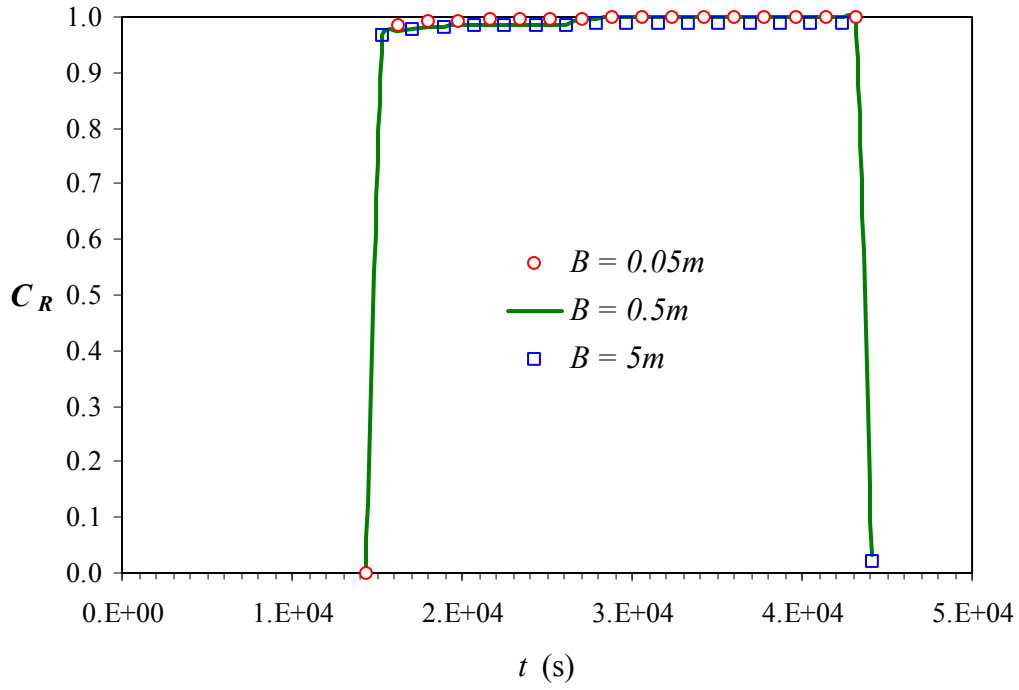


Figure 3a. Breakthrough curves for three different B values at $t_T = 0.5 t_i$.

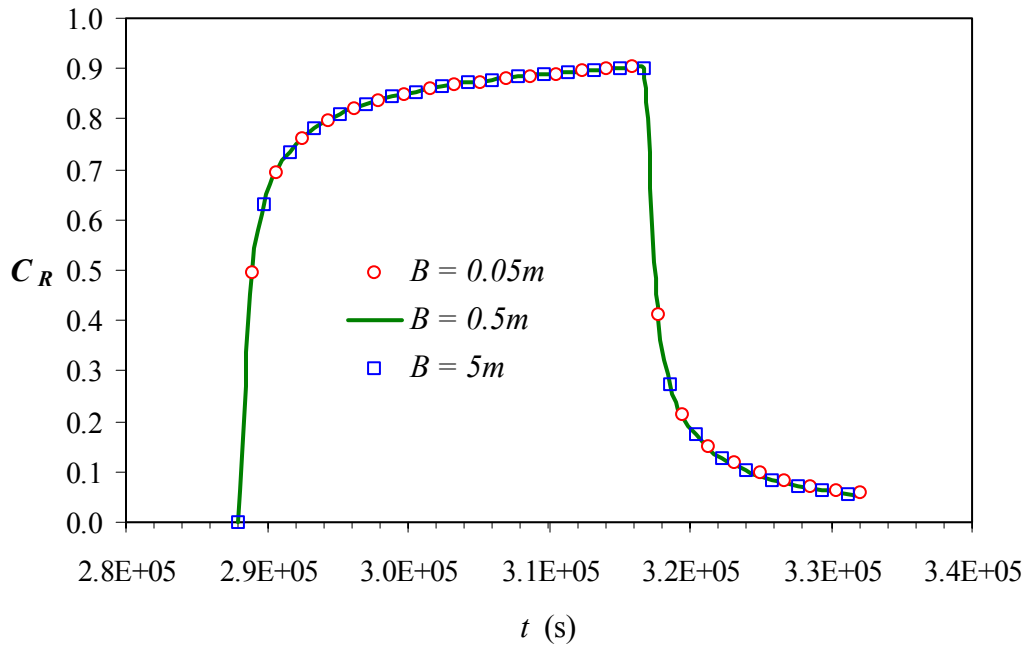


Figure 3b. Breakthrough curves for three different B values at $t_T = 10 t_i$.

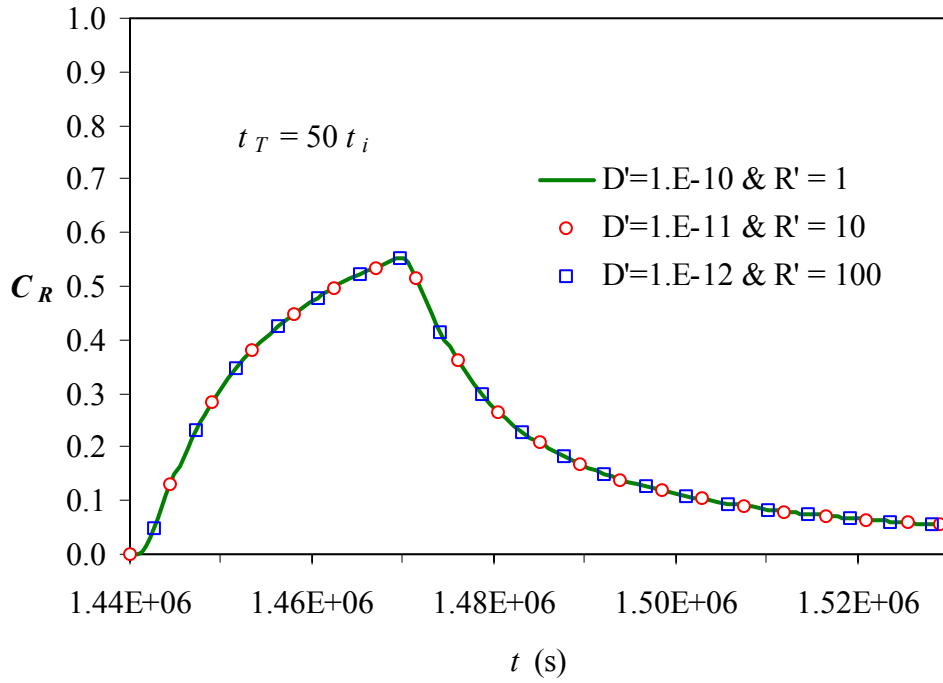


Figure 4. Breakthrough curves for three different combinations of D' (m^2/s) and R' .

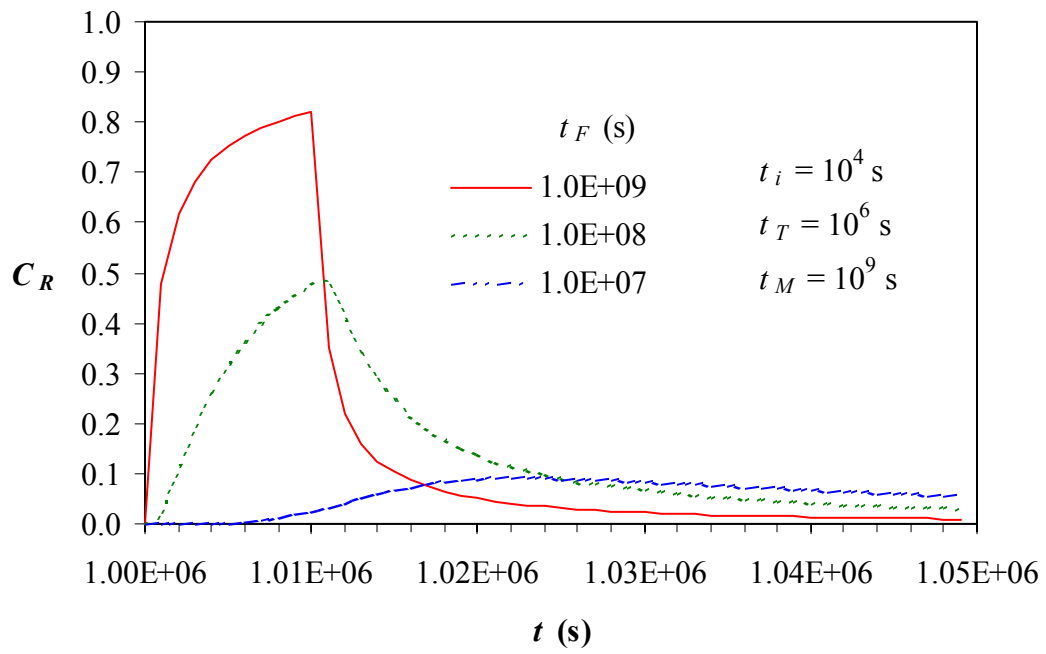


Figure 5. The effect of t_F on breakthrough curves.

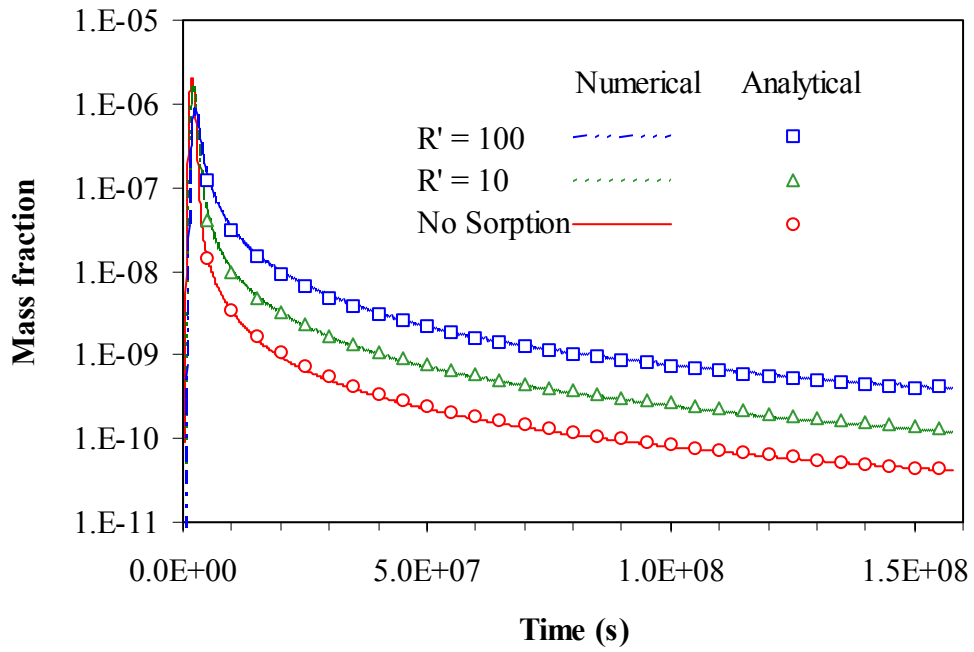


Figure 6. Comparison of the analytical solution with the numerical (TOUGH2) solution.

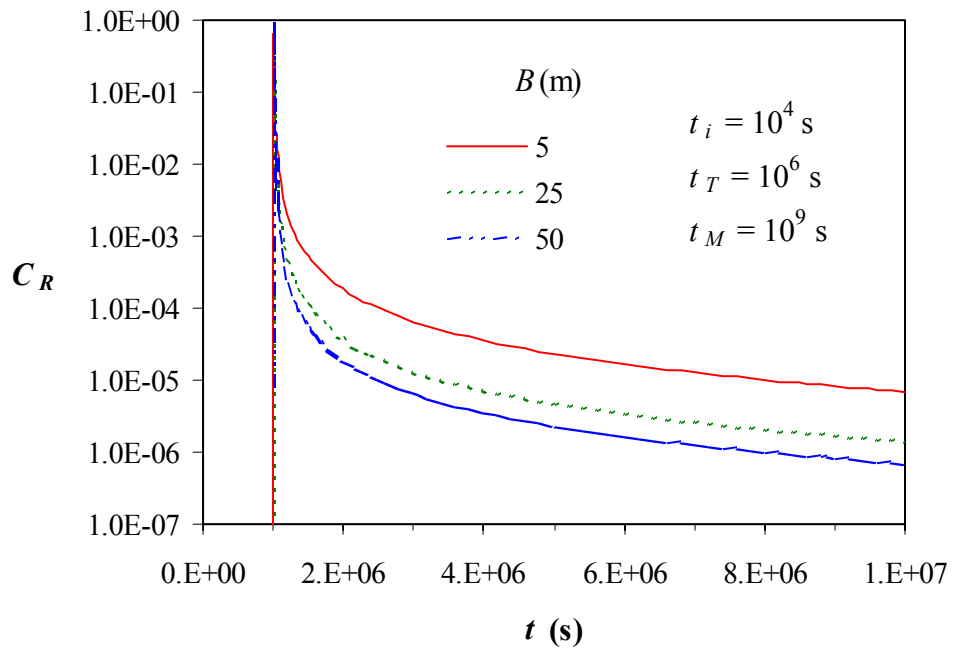


Figure 7. The effect of fracture spacing on BTC.